

## THERMAL DECOMPOSITION AND CREATION OF REACTIVE SOLID SURFACES. IV. EFFECT OF $\text{NH}_4\text{NO}_3$ INCLUSION ON THE THERMAL GENESIS OF CHROMIA CATALYST FROM A PARENT GEL

M.I. ZAKI \* and N.E. FOUAD

*Chemistry Department, Faculty of Science, Minia University, El-Minia (Egypt)*

(Received 3 May 1985)

### ABSTRACT

The effect of  $\text{NO}_3^-$  contaminant on the thermal decomposition of chromia gel has been thoroughly investigated.  $\text{NO}_3^-$ -free gel, prepared by treating a dilute solution of chromium nitrate with aqueous ammonia, and a simulated  $\text{NO}_3^-$ -contaminated one, obtained by mechanically mixing calculated amounts of the pure gel and  $\text{NH}_4\text{NO}_3$  (4.7–33.3% by weight), have been subjected to thermogravimetric and differential thermal analyses. The thermal behaviour thus monitored has been physicochemically characterized by means of infrared and X-ray diffraction techniques. The results obtained have revealed a notable disparity between the reaction pathways conceded by the pure and the contaminated gel yielding chromias of different properties.

### INTRODUCTION

It has become evident that adsorptive [1,2], redox catalytic [3,4] and semiconductive properties [3,5,6] of calcined chromia are largely interrelated and governed by both the nature and degree of surface nonstoichiometry (existence of excess oxygen associated with surface Cr ions of valency  $> 3 +$  up to  $6 +$ ). Within this context a number of investigations [2,3,7,8], devoted solely to exploring the physicochemical attributes of chromia surface nonstoichiometry, have clearly demonstrated its strong dependence on the preparation conditions applied.

As far as preparation conditions are concerned, the thermal decomposition of unsupported or supported inactive precursor (e.g., chromia gel [1–3,9],  $(\text{NH}_4)_2\text{Cr}_2\text{O}_7$  [2,10] and  $\text{CrO}_3$  [2,11]) has been proved to be the most preferable method. On the other hand, chromia gel (prepared by treating a dilute solution of  $\text{Cr}(\text{NO}_3)_3 \cdot 9\text{H}_2\text{O}$  with base) has been the

---

\* To whom all correspondence should be forwarded at the present address: Institut Für Physikalische Chemie, Universität München, Sophienstrasse 11, 8000 München 2, F.R.G.

favourite precursor [9], for it leads to high-surface-area unsupported chromia catalysts [2] and facilitates the preparation of highly dispersed supported ones [7]. It is worth mentioning that the preparation of supported catalysts by such a coating method is believed to result in a more extensive two-dimensional distribution of the catalyst precursor on the support surface (monolayer-type), as compared to the supported catalysts obtained via the conventional impregnation method [7]. This is simply because the coating method loads the catalyst precursor by deposition, thus neutralizing the role of the support surface chemistry in governing its primary interaction with an ionic precursor being impregnated from an aqueous medium [12,13].

However, the trouble with chromia gel is that it may retain appreciable amounts of ammonium nitrate (formed as a secondary product of the precipitation reaction) due to either a prohibited wash-off (in order not to disturb the homogeneous coating of a supported gel) or to an insufficient wash-off (dealing with an unsupported one). The oxidizing power of retained  $\text{NO}_3^-$  would somehow intervene, throughout the course of the gel thermal decomposition, by attacking nearby chromium ions and/or by contributing dominantly to the total surface oxidation power of the catalyst yielded [7].

The present paper accounts for a thermoanalytical investigation of the effect of  $\text{NH}_4\text{NO}_3$  inclusion on the thermal genesis of chromia catalysts from a parent gel. To accomplish this objective, a thorough physicochemical characterization of various events encountered throughout the course of the overall process has been performed by means of infrared and X-ray diffraction techniques.

## EXPERIMENTAL

### *Materials*

Chromia gel was prepared [9] by adding 0.3 M ammonia solution dropwise to 0.1 M chromium nitrate solution, with constant stirring, until complete precipitation at pH 9.2. The gel was left overnight, then filtered and washed thoroughly with warm distilled water until  $\text{NO}_3^-$ -free. Drying was effected at 80°C to constant weight (72 h). The water content of the dried gel (ca. 37.5% by weight) was found to correspond to the approximate composition  $\text{Cr}_2\text{O}_3 \cdot 5\text{H}_2\text{O}$ . Preliminary X-ray diffraction analysis revealed an amorphous nature for the gel.  $\text{NO}_3^-$ -contaminated gel samples were simulated by mechanically mixing calculated amounts of  $\text{NH}_4\text{NO}_3$  salt and the gel, using an electric mill (SPECAC) provided with agate balls, for 2 h. The homogeneous mixtures thus obtained were kept dry over  $\text{P}_2\text{O}_5$ . The range of mixing was designed to provide samples of various contamination levels (4.7–33.3% by weight). Samples subjected to IR and X-ray analyses were obtained by calcination of independent portions of the pure and a

contaminated gel (obtained at 28.5% level) at various temperatures (110–450°C) for 2 h. They are notified, respectively, by Gel and Gen, followed by the parenthesized calcination temperature. For example, Gel(400) notifies the calcination product of the  $\text{NO}_3^-$  free gel at 400°C for 2 h, whereas Gen(210) indicates that obtained from the 28.5%-contaminated gel at 210°C for 2 h. All chemicals used in the preparations and those employed as reference materials ( $(\text{NH}_4)_2\text{CrO}_4$ ,  $(\text{NH}_4)_2\text{Cr}_2\text{O}_7$ ,  $\text{CrO}_3$  and  $\alpha\text{-Cr}_2\text{O}_3$ ) were high purity (99.8%) Merck products.

### *Apparatus and techniques*

Thermogravimetric (TG) and differential thermal analysis (DTA) curves were automatically recorded over a wide range of temperature (1000°C), at a heating rate standardized at  $10^\circ\text{C min}^{-1}$ , in a dynamic atmosphere of air (15 ml  $\text{min}^{-1}$ ), using small portions of test samples (10–15 mg), by means of the apparatus (Shimadzu thermal analyser, Japan) and techniques described earlier [14]. It is worth mentioning that sample cells were provided with fine-perforated lids to prevent the sweeping-out of test sample particles. The X-ray diffraction analyses (XRD), using Ni-filtered  $\text{Cu K}\alpha$  radiation, and IR absorption (IRA) of thin discs of KBr-supported test samples were performed on the pure and contaminated gel as well as their calcination products (110–450°C) employing the apparatus and adopting the techniques detailed earlier [15].

## RESULTS AND DISCUSSION

### *Characterization of the thermal decomposition course of $\text{NO}_3^-$ -free chromia gel (Gel)*

TG and DTA curves of the Gel sample are included in Figs. 1 and 2, respectively, whereas the IR spectra of its calcination products (at 110–450°C) are exhibited in Fig. 3.

The TG curve (Fig. 1) demonstrates that the Gel sample suffers a gradual weight loss of ca. 38.0% through, apparently, a single step occurring at 50–310°C. The product thus yielded shows a notable thermal stability at 310–370°C, then suffers a slight weight loss, as the temperature reaches 380°C, bringing the total loss up to 45.0%. The corresponding DTA curve (Fig. 2), however, reveals a composite nature for this step (50–315°C), by monitoring two endothermic processes (centred around 100 and 185°C) succeeded by three overlapping exothermic processes maximized at 230, 280 and 330°C. It further monitors a strong, sharp exothermic process occurring (at 405°C) immediately beyond the second weight loss step.

Gravimetric calculations, based on the results determined by the TG curve (Fig. 1), suggested that the early endothermic weight loss process (14.0%), at

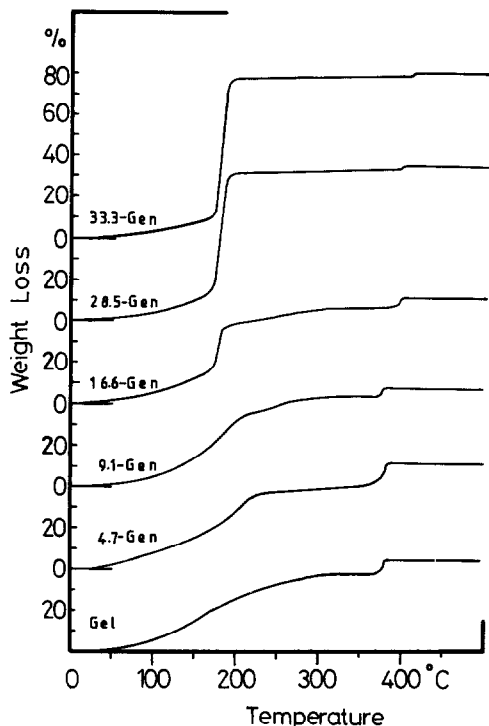


Fig. 1. TG curves for the  $\text{NO}_3^-$ -free (Gel) as well as the contaminated (Gen) gel samples.

50–150°C, involves the elimination of two water molecules (14.8%), leading to the formation of an intermediate trihydrate, viz.  $\text{Cr}_2\text{O}_3 \cdot 3\text{H}_2\text{O}$ . They further suggest that the following endothermic weight loss process (ca. 28.0%), at 150–210°C, involves the elimination of another two water molecules (29.7%) resulting in the formation of an intermediate monohydrate, viz.  $\text{Cr}_2\text{O}_3 \cdot \text{H}_2\text{O} \approx 2\text{CrOOH}$ . The calcination products obtained in the temperature range in which the gel dehydrates, i.e., 110–210°C, were still amorphous to XRD. However, radial electron distribution measurements (RED), performed by Ratnasamy and Leonard [16], have indicated the existence of short-range structures, similar to  $\text{CrOOH}$ , in chromia gel calcined at 210°C.

The IR spectrum of the gel, which is partly exhibited (1200–200  $\text{cm}^{-1}$ ) in Fig. 3, displayed various absorptions over the normal range of water vibrations (3800–1500  $\text{cm}^{-1}$ ), manifesting the existence of various types of retained water, namely dissociatively ( $\nu\text{OH}$  at 3510  $\text{cm}^{-1}$ ) and nondissociatively adsorbed ( $\nu\text{OH}$  at 3420  $\text{cm}^{-1}$  +  $\delta\text{OH}$  at 1620  $\text{cm}^{-1}$ ), and coordinated water molecules ( $\delta\text{OH}$  at 1590  $\text{cm}^{-1}$ ). These assignments are in accord with Zecchina et al. [17]. Upon calcination to 150°C, the bands at 1620 and 1590  $\text{cm}^{-1}$  were completely eliminated, whereas that at 3420  $\text{cm}^{-1}$  was drastically weakened. These modifications indicate that the 1st endothermic weight loss step (Fig. 1) involves the removal of physisorbed as well as coordinated

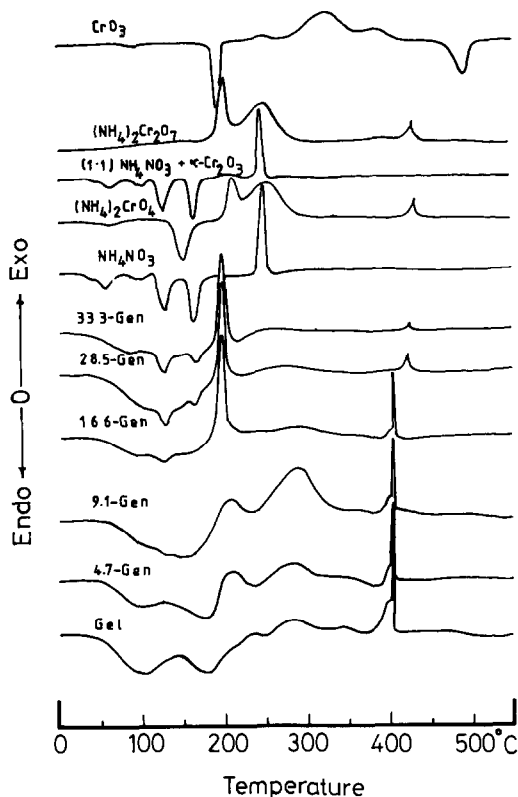


Fig. 2. DTA curves for the  $\text{NO}_3^-$ -free (Gel) as well as the contaminated (Gen) gel samples. Reference curves inset for comparison.

water molecules. A further increase of the calcination temperature to  $210^\circ\text{C}$  caused an almost complete disappearance of the absorptions at  $3510$  and  $3420\text{ cm}^{-1}$ , and created a weak, but broad, absorption centred around  $1650\text{ cm}^{-1}$ . This must mean that the 2nd endothermic weight loss (Fig. 1) involves the complete removal of loosely bound water molecules. On the other hand, the absorption created around  $1650\text{ cm}^{-1}$  cannot be assigned to the bending mode of hydroxyl groups, simply because of the absence of the corresponding stretch at  $3800\text{--}3300\text{ cm}^{-1}$ . Crystalline  $\text{CrOOH}$  exhibits [18] a similar, very broad IR absorption at  $1640 \pm 30\text{ cm}^{-1}$ , due to O-H stretching vibrations in OHO groups. Compatibly, the simultaneously developed strong absorption at  $930\text{ cm}^{-1}$ , in the spectra of Gel (190) and (210) (Fig. 3), could well be considered for the relevant terminal Cr-O vibrations [17]. These results, sustained by the reported RED findings [16], presume the formation of  $\text{CrOOH}$ -like short-range structures at  $> 150\text{--}210^\circ\text{C}$ .

The TG curve (Fig. 1) further shows that the gel keeps losing weight gradually up to  $310^\circ\text{C}$ , where a product of notable thermal stability (at  $310\text{--}370^\circ\text{C}$ ) is yielded. The corresponding DTA curve (Fig. 2), however,

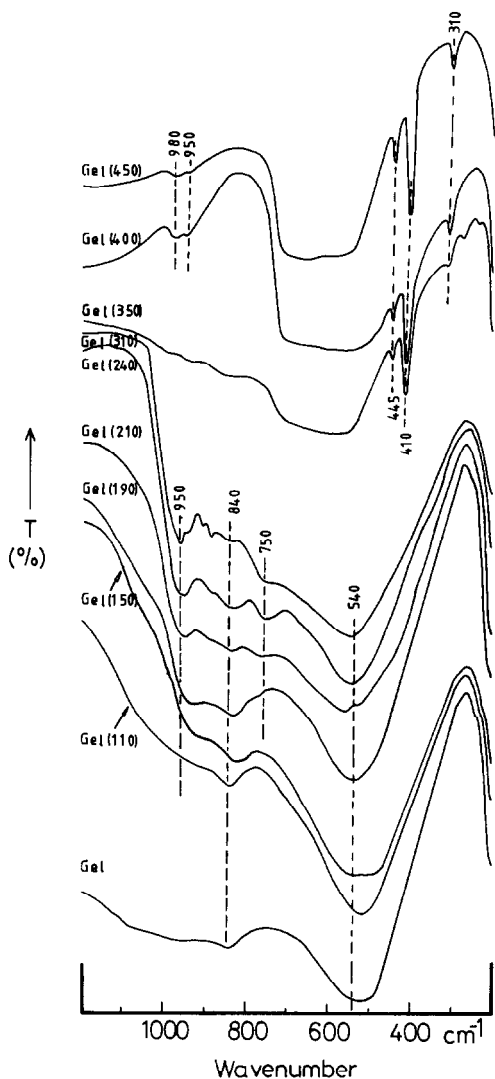


Fig. 3. IR spectra from the  $\text{NO}_3^-$ -free gel and its calcination products at the temperatures indicated.

displays no relevant endothermic effects. It shows instead a composite broad exothermic effect over a wide range of temperature (230–340°C). It is most likely that this exothermic effect was strong enough to completely compensate the anticipated endothermic ones. It is worth mentioning that this exothermic effect has been considered [19] to mark the oxidation of the gel. Our earlier surface investigation of calcined chromia gel [2] has compatibly allocated the maximum content of surface excess charge ( $\text{Cr}^{>3+-6+}$ ) to products obtained at 250–300°C.

Zecchina et al. [17] have assigned IR absorptions in the region 1000–700  $\text{cm}^{-1}$  to surface groups of the  $\text{CrO}_4^{x-}$ -type, where  $x = 2, 3$  or 4. Such

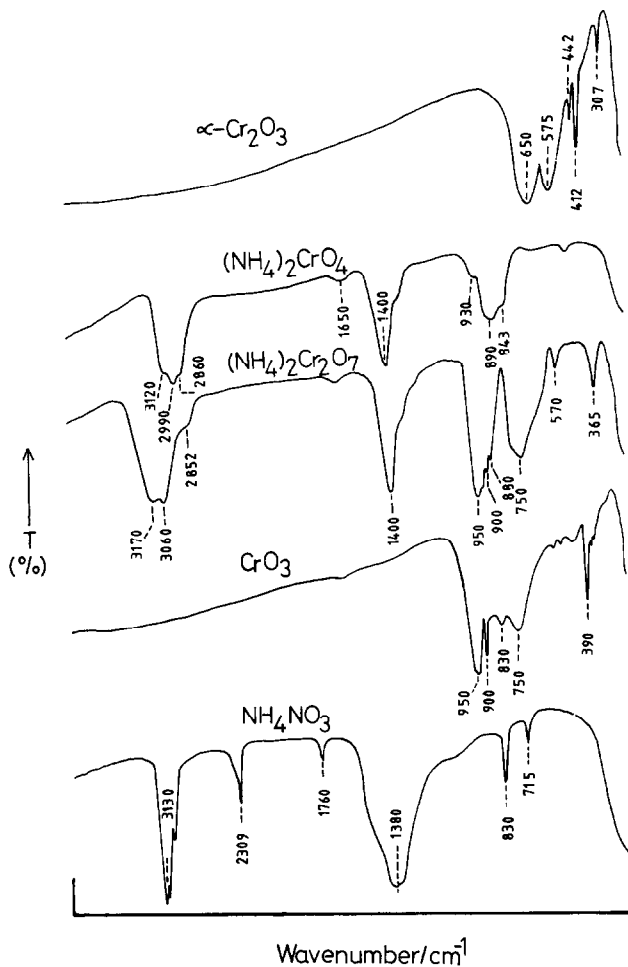


Fig. 4. Reference IR spectra.

absorptions do not show up clearly in our spectra before the calcination temperature reaches  $190^\circ\text{C}$  (Fig. 3), then they develop markedly on increasing temperature up to  $310^\circ\text{C}$ . A close inspection of the absorptions at  $1000\text{--}700\text{ cm}^{-1}$  in the spectrum of Gel (190) reveals the existence of two bands at  $930$  and  $830\text{ cm}^{-1}$ . These bands are normally assigned to terminal Cr–O stretching vibrations associated with isolated  $\text{CrO}_4^{2-}$  tetrahedrons [20] (cf. the reference spectrum of  $(\text{NH}_4)_2\text{CrO}_4$  given in Fig. 4). As the calcination temperature increases to  $310^\circ\text{C}$ , these bands shift to higher frequencies (namely to  $950$  and  $840$ , respectively) and a new one emerges at  $750\text{ cm}^{-1}$ . These IR absorptions can be seen in Fig. 4 characterizing the chromium–oxygen vibrations of  $(\text{NH}_4)_2\text{Cr}_2\text{O}_7$  or  $\text{CrO}_3$ . More precisely, they account for a polymerization process involving the isolated  $\text{CrO}_4^{2-}$  tetrahedra. As a matter of fact, the band at  $750\text{ cm}^{-1}$  is diagnostic for the

antisymmetric stretch of Cr–O–Cr bridges consequently formed [20]. Polychromates normally result from the sharing of vertices between certain numbers of  $\text{CrO}_4$  tetrahedra [21]. As Cr–O–Cr bridges form, the bond length of the terminal Cr–O decreases (viz.  $(1.66 \text{ \AA})\text{CrO}_4^{2-} \rightarrow (1.63 \text{ \AA})\text{Cr}_2\text{O}_7^{2-} \rightarrow (1.60 \text{ \AA})\text{CrO}_3$  [21]), presumably due to a corresponding increase in the degree of covalency, the quantity which justifies the observed high-frequency shift of the relevant absorptions.

Based on the results reported above, one may infer that  $\text{CrOOH}$  has been a target for an intensive oxidation process since its early formation in the immediate vicinity of  $190^\circ\text{C}$ . Indeed, Franco and Sing [22] have supported the possibility of the formation of  $\text{CrO}_2$  as an oxidation product of the oxyhydroxide, according to the equation:  $\frac{1}{2}\text{O}_2 + \text{CrOOH} \rightarrow \text{CrO}_2 + \text{H}_2\text{O}$ . Accordingly, a similar topochemical reaction, also being accompanied by a weight loss (dehydration), can be adopted for the initial oxidation of the gel maximized at  $230^\circ\text{C}$  (Fig. 2).

The further oxidation of  $\text{CrO}_2$  to the chromates is most likely responsible for the successive exothermic process maximized at  $280^\circ\text{C}$  (Fig. 2). As the local density of chromates increases, i.e., become closely situated, the subsequent polymerization occurs giving rise to the consistent IR characteristics monitored for Gel(240) and (310). Since these calcination products were still amorphous to XRD, they should be considered to represent amorphous chromia-supported polychromates, i.e., the successive oxidation processes are confined to a limited proportion of the gel. In fact, the characteristic IR absorption of the gel at  $540 \text{ cm}^{-1}$  is consistently displayed for the calcination products obtained at  $110$ – $310^\circ\text{C}$ . On further heating to  $350^\circ\text{C}$ , the first notable departure from the IR band structure occurs at  $< 750 \text{ cm}^{-1}$ . XRD provided a markedly noisy diffractogram of rather weak and fuzzy lines at  $4.20$ ,  $3.40$ ,  $2.86$ ,  $2.36$  and  $2.25 \text{ \AA}$  for Gel(350). Accordingly [23], such a pattern could account for poorly crystalline  $\text{Cr}_2\text{O}_3 \cdot \text{CrO}_3$  as being the thermally stable phase at  $\geq 310$ – $370^\circ\text{C}$ . The IR spectrum of Gel(350), given in Fig. 3, monitors the coexistence of absorptions of chromates ( $1000$ – $700 \text{ cm}^{-1}$ ) and “ $\text{Cr}_2\text{O}_3$ -like” structures ( $700$ – $300 \text{ cm}^{-1}$  [24]). It is worth mentioning that a number of oxides and compounds containing  $\text{Cr}^{\text{III}}$  and  $\text{Cr}^{\text{VI}}$  have been successfully prepared [21] via the thermal decomposition of  $\text{CrO}_3$  or a thermally assisted solid-state reaction between polychromates and  $\text{CrO}_3$  in an oxidizing atmosphere, e.g.,  $\text{Cr}_5\text{O}_{12} \approx \text{Cr}_2^{\text{III}}(\text{Cr}^{\text{VI}}\text{O}_4)_3$  and  $\text{Cr}_3\text{O}_8^- \approx [\text{Cr}^{\text{III}}(\text{Cr}^{\text{VI}}\text{O}_4)_2]^-$ . They are believed to be formed via complex series of exothermic disproportionation reactions involving  $\text{Cr}^{\text{V}}$  and  $\text{Cr}^{\text{IV}}$  species [21]. The coexistence of such oxidation states was magnetically as well as optically detected, by Ellison and Sing [8], for a series of chromias calcined at  $200$ – $600^\circ\text{C}$ .

Upon increasing the temperature up to  $390^\circ\text{C}$ ,  $\text{Cr}_2\text{O}_3 \cdot \text{CrO}_3$  begins to lose its stability undergoing a 9.5% loss of its original weight, as determined from the TG curve (Fig. 1). It is plausible to presume beforehand that this loss is



primarily due to released oxygen, for the IR spectrum of Gel(350) declared its anhydrous nature. Gravimetrically, this loss (9.5%) equals what one would expect from  $2\text{Cr}_2\text{O}_3 \cdot \text{CrO}_3 \rightarrow 3\text{Cr}_2\text{O}_3 + \frac{1}{2}\text{O}_2$ . The strong sharp exothermic effect which immediately follows at  $405^\circ\text{C}$ , known as the “glow phenomenon” [19], is diagnostic for the crystallisation of  $\alpha\text{-Cr}_2\text{O}_3$ .

The IR spectra of Gel(400) and (450), exhibited in Fig. 3, reveal the formation of  $\alpha\text{-Cr}_2\text{O}_3$  (absorptions at  $700\text{--}500$ ,  $445$ ,  $410$  and  $310\text{ cm}^{-1}$  [24]) having “oxygen-rich” surfaces (absorptions at  $1000\text{--}900\text{ cm}^{-1}$  [9,17]). However, the ill-resolved strong absorption at  $700\text{--}500\text{ cm}^{-1}$ , as compared to that displayed in the reference spectrum of typical  $\alpha\text{-Cr}_2\text{O}_3$  (Fig. 4), may be due to the fact (XRD verified) that these calcination products are not sufficiently crystalline. Earlier investigations [2] proved that well-crystalline  $\alpha\text{-Cr}_2\text{O}_3$  can be obtained only after prolonged calcination of the gel at  $\geq 700^\circ\text{C}$ .

#### *The thermal decomposition course of $\text{NH}_4\text{NO}_3$*

The thermal behaviour of anhydrous  $\text{NH}_4\text{NO}_3$  is shown by the DTA curve included in Fig. 2. It involves four endothermic processes ( $55$ ,  $85$ ,  $127$  and  $170^\circ\text{C}$ ) and an exothermic one ( $245^\circ\text{C}$ ). These results are identical to those reported elsewhere [25]. The first three endothermic processes are ascribed to consecutive series of phase transformations (their identifications are reviewed elsewhere [26]), whereas the one that follows at  $170^\circ\text{C}$  marks the melting of the salt. On the other hand, the exothermic effect at  $245^\circ\text{C}$  was found to correspond to the salt decomposition. Thermogravimetric analysis showed that the salt commences to lose weight at  $230^\circ\text{C}$  to ca. 100% weight loss at  $250^\circ\text{C}$  via a single, distinct step.

#### *Characterization of the thermal decomposition course of $\text{NO}_3^-$ -contaminated chromia gel (Gen)*

$\text{NO}_3^-$ -contaminated chromia gel samples were simulated by preparing homogeneous mechanical mixtures of the gel and  $\text{NH}_4\text{NO}_3$ , at various contamination levels ( $4.7\text{--}33.3\%$ ), as detailed in the Experimental section. TG and DTA curves obtained for this set of samples are exhibited in Figs. 1 and 2, respectively. Relevant reference DTA curves are also given in Fig. 2. IR spectra from the various calcination products ( $110\text{--}450^\circ\text{C}$ ) of the gel contaminated at  $28.5\%$  (notified by Gen) are exhibited in Fig. 5.

The TG curve (Fig. 1) of the 4.7-Gen sample reflects a behaviour slightly different from that exhibited for the  $\text{NO}_3^-$ -free gel (Gel). An ill-defined weight loss step emerges at ca.  $210^\circ\text{C}$ . The DTA curve monitors a corresponding exothermic effect at  $210^\circ\text{C}$ , and a notable development of the exothermic effect at  $280^\circ\text{C}$  (Fig. 2). These developments are intensified, besides the emergence of additional endothermic contributions at  $127$  and  $150^\circ\text{C}$ , upon increasing the contamination level to  $9.1\%$ .

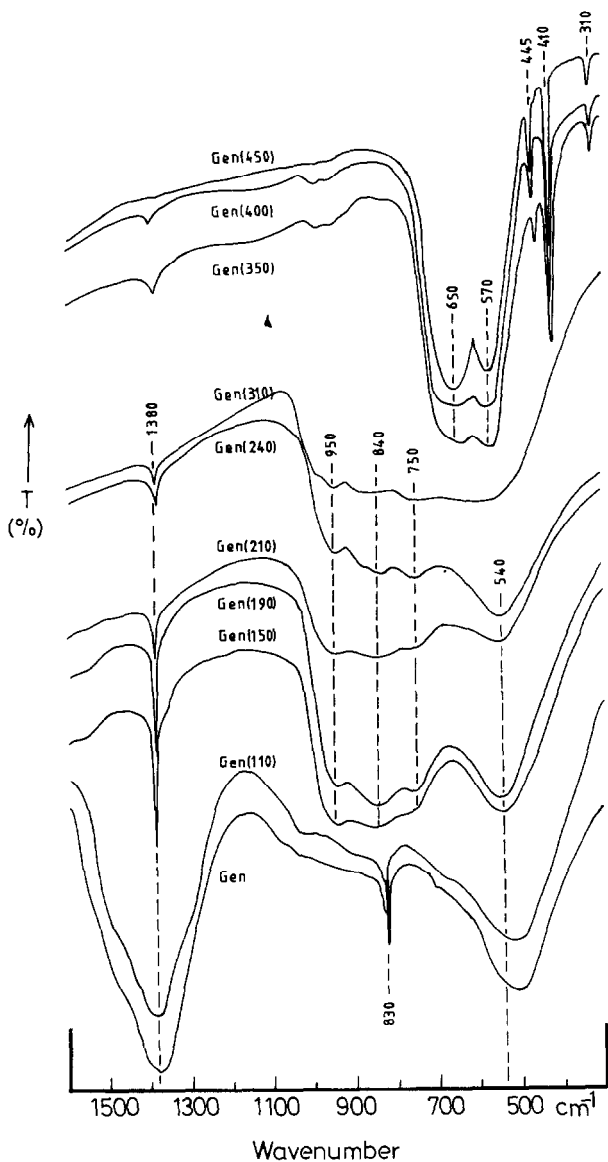


Fig. 5. IR spectra from the  $\text{NO}_3^-$ -contaminated gel (at 28.5% level) and its calcination products at the temperatures indicated.

A further increase in the contamination level (> 9.1 to 33.3%) has caused a dramatic departure from the thermal behaviour of the  $\text{NO}_3^-$ -free gel (Gel) as shown in Figs. 1 and 2. This is manifested in the simultaneous increase in the weight loss at 210°C, with a gradual shift of the location of its maximum rate to lower temperatures (namely from 210 (4.7%) to ca. 180°C (33.3%)). Moreover, the weight loss at 380°C decreases simultaneously, whereas its maximum rate shifts to higher temperatures (namely, from 380 (4.7%) to

415°C (33.3%). Consistent changes are monitored by the corresponding DTA curve (Fig. 2): a gradual increase in the intensity of the endothermic effects at 127 and 170°C; a marked increase in the intensity of the exothermic effect at 180°C (initially located at 210°C); a decrease in the amount of heat released at 280°C to almost complete diminution; and a parallel drastic deterioration of the amount of heat released at 405°C with a forward shift to ca. 425°C.

A close inspection of the results described above leads to the following inferences:

(i) The absence of the exothermic effect (at 245°C) that marks the decomposition of  $\text{NH}_4\text{NO}_3$ , though other relevant genuine effects are monitored (viz. endothermic effects at 127 and 170°C, Fig. 2), may suggest earlier decomposition of the salt, presumably, via a different mechanism. The IR spectra from the parent Gen sample (28.5%) and its calcination product at 110°C (Fig. 5), lose the characteristic absorptions of the loaded  $\text{NH}_4\text{NO}_3$  (i.e., bands at 1380, 830 and 715  $\text{cm}^{-1}$ , as assigned by the reference spectrum given in Fig. 4) upon increasing the calcination temperature to 150°C. It is worth mentioning that the sharp band at 1380  $\text{cm}^{-1}$ , which persists with the increase in temperature to 400°C (Fig. 5), presumably arises from surface  $\text{NO}_3^-$  species;

(ii) The newly emerged exothermic effect at 210°C (Fig. 2), which shifts to 180°C at contamination levels > 9.1%, is consistent with the distinct weight loss step maximized at 180°C (Fig. 1). The IR spectra given (Fig. 5) for Gen (150) and (190) display strong absorptions due to polychromates (at 1000–700  $\text{cm}^{-1}$ ), which are not monitored for the corresponding calcination products of the Gel sample (Fig. 3). These results, together with the fact that the thermal effect concerned takes place at a temperature (180°C) just intermediate between the temperature (150°C) at which  $(\text{NH}_4)_2\text{CrO}_4$  endothermically transforms to  $(\text{NH}_4)_2\text{Cr}_2\text{O}_7$  [23,27], and that (210°C) at which the latter exothermically decomposes [23] (as controlled by the relevant reference DTA curves given in Fig. 2), suggest that the exothermic effect at 180°C is associated with the decomposition (Fig. 1) of an oxidation product, probably dichromate-like.

(iii) The almost complete disappearance of the strong exothermic effect at 280°C (assigned to  $\text{NO}_3^-$ -free gel oxidation), though the IR spectra of Gen (210), (240) and (310) still give strong evidence for the existence of surplus polychromates (Fig. 5), may implicitly account for a retrogression of the role undertaken by atmospheric oxygen in the upsurged oxidation of the gel. Moreover, the parallel deterioration of the glow phenomenon at 405°C (Fig. 2), though an evident earlier formation of  $\alpha\text{-Cr}_2\text{O}_3$  is explicitly shown by the IR spectrum of Gen (350) (Fig. 5), which was further supported by XRD, undoubtedly proves that crystallisation of chromia from an amorphous parent no longer exists.

Within the above context, it is clear that  $\text{NH}_4\text{NO}_3$  contaminant forces the

thermal decomposition of chromia gel to modify its course. According to the information put forward by the present investigation, it seems that the  $\text{NO}_3^-$  contained supplies the intermediate  $\text{CrOOH}$  with surplus active oxygen, in the immediate vicinity of its formation.

The  $\text{NO}_3^-$ -initiated oxidation of the gel, at a temperature as low as  $150^\circ\text{C}$ , would lead firstly to the formation of isolated  $\text{CrO}_4^{2-}$  species, which would then polymerize into clusters of dichromate species. Such a presumption may find solid ground from the fact that  $(\text{NH}_4)_2\text{Cr}_2\text{O}_7$  decomposes at  $210^\circ\text{C}$  to a product which gives rise to a small exothermic effect at  $425^\circ\text{C}$  (reference DTA curve in Fig. 2), comparable to the thermal behaviour of the 28.5 or 33.3% contaminated gel at  $210\text{--}450^\circ\text{C}$  (Fig. 2).

As far as the decomposition of ammonium dichromate is concerned, it was believed [28] to proceed according to the reaction



However, a recent mass spectrometric determination of the reaction gaseous products [29] has proved the formation of  $\text{N}_2$ ,  $\text{N}_2\text{O}$  and  $\text{H}_2\text{O}$  through the oxidation of  $\text{NH}_3$  on nearby freshly generated  $\text{CrO}_3$  surfaces. This must lead to an immediate reduction of  $\text{Cr}^{\text{VI}}$  to lower valencies. Earlier XRD results [2] have indicated the formation of crystalline  $\alpha\text{-Cr}_2\text{O}_3$  by decomposing  $(\text{NH}_4)_2\text{Cr}_2\text{O}_7$  at  $300^\circ\text{C}$ . It is thus understandable why the reducing effect involved is shown (Fig. 2) to be dependent on the amount of  $\text{NH}_4\text{NO}_3$  contained, viz. at  $\geq 28.5\%$  contamination level. The reference DTA curve given in Fig. 2 for a 1:1 mixture of  $\text{NH}_4\text{NO}_3$  and  $\alpha\text{-Cr}_2\text{O}_3$  only monitors the genuine thermal behaviour of the salt. This may lend a further strong support to that  $\text{CrOOH}$  is an indispensable oxygen-tolerant intermediate for the gel oxidation.

In conclusion, the contamination with  $\text{NH}_4\text{NO}_3$ , at an appreciable level ( $\geq 28.5\%$ ), accelerates the thermal genesis of well-crystallised  $\alpha\text{-Cr}_2\text{O}_3$ . This can be realized by comparing the IR spectra of the calcination products of the Gen and Gel samples at  $> 350^\circ\text{C}$  (Figs. 5 and 3, respectively), with reference to the spectrum given in Fig. 4 for typical  $\alpha\text{-Cr}_2\text{O}_3$ . Clusters of dichromate species are presumed to be the intermediate for such an accelerated genesis of  $\alpha\text{-Cr}_2\text{O}_3$  from the Gen sample. An earlier analytical investigation of surface excess oxygen on chromias obtained by the thermal decomposition of a  $\text{NO}_3^-$ -free gel or  $(\text{NH}_4)_2\text{Cr}_2\text{O}_7$  has indicated [2] that the former precursor yields highly nonstoichiometric chromias as compared to the latter. If, according to McDaniel and Burwell [7], the greater the quantity of excess oxygen, the larger the pore diameter and the smaller the surface area, the presence of  $\text{NO}_3^-$  contaminant would lead to chromia catalysts of differing surface properties.

## REFERENCES

- 1 F.S. Baker, J.D. Carruthers, R.E. Day, K.S.W. Sing and L.J. Stryker, *Discuss. Faraday Soc.*, 52 (1971) 173.
- 2 R.B. Fahim, R.M. Gabr, M.I. Zaki and S.A.A. Mansour, *J. Colloid Interface Sci.*, 81 (1981) 468; R.B. Fahim, M.I. Zaki and N.H. Yacoub, *J. Colloid Interface Sci.*, 88 (1982) 502.
- 3 J. Deren, J. Haber, H. Podgorecka and J. Burzyk, *J. Catal.*, 2 (1963) 161.
- 4 R.B. Fahim, M.I. Zaki and R.M. Gabr, *Appl. Catal.*, 4 (1982) 189.
- 5 S.R. Morrison, *J. Catal.*, 47 (1977) 69; *Chemtech*, 7 (1977) 570.
- 6 R.B. Fahim, R.M. Gabr and M.I. Zaki, *Indian J. Chem.*, 19A (1980) 829.
- 7 M.P. McDaniel and R.L. Burwell, Jr., *J. Catal.*, 36 (1975) 394, 404.
- 8 A. Ellison and K.S.W. Sing, *J. Chem. Soc., Faraday Trans.*, 1, 74 (1978) 2807.
- 9 R.L. Burwell, Jr., G.L. Haller, K.C. Taylor and J.F. Read, *Adv. Catal.*, 20 (1969) 1.
- 10 P.J.M. Carrott and N. Sheppard, *J. Chem. Soc., Faraday Trans. 1*, 79 (1983) 2425.
- 11 M.P. McDaniel, *J. Catal.*, 76 (1982) 37.
- 12 G.A. Parks, *Chem. Rev.*, 65 (1965) 177.
- 13 W.K. Hall, *Proc. Climax 4th Int. Conf. on Chemistry and Uses of Molybdenum*, Climax Molybdenum Company, Ann Arbor, MI, 1982, p. 224.
- 14 R.B. Fahim, M.I. Zaki and G.A.M. Hussien, *Powder Technol.*, 30 (1982) 161.
- 15 R.B. Fahim, M.I. Zaki and R.M. Gabr, *Surf. Technol.*, 11 (1980) 215.
- 16 P. Ratnasamy and A.J. Leonard, *J. Phys. Chem.*, 76 (1972) 1838.
- 17 A. Zecchina, S. Coluccia, E. Guglielminotti and G. Ghiotti, *J. Phys. Chem.*, 75 (1971) 2774.
- 18 R.G. Snyder and J.A. Ibers, *J. Chem. Phys.*, 36 (1961) 1356.
- 19 J.D. Carruthers, K.S.W. Sing and J. Fenerty, *Nature (London)*, 213 (1967) 66.
- 20 J.A. Campbell, *Spectrochim. Acta*, 21 (1965) 1333.
- 21 A.F. Wells, *Structural Inorganic Chemistry*, 3rd edn., Clarendon Press, London, 1978, pp. 945-947.
- 22 M. A. Alario Franco and K.S.W. Sing, *J. Therm. Anal.*, 4 (1972) 47.
- 23 H. Park, *Bull. Chem. Soc. Jpn.*, 45 (1972) 2749.
- 24 R. Marshall, S.S. Mitra, P.J. Gielisse, J.N. Plende and L.C. Mansur, *J. Chem. Phys.*, 43 (1965) 2893.
- 25 L. Erdey, S. Gal and G. Liptay, *Talanta*, 11 (1969) 913.
- 26 A.C. McLaren, *Rev. Pure Appl. Chem.*, 12 (1962) 54.
- 27 S. Rajam and A.K. Galwey, *J. Chem. Soc., Faraday Trans. 1*, 78 (1982) 2553.
- 28 R.B. Heslop and P.L. Robinson, *Inorganic Chemistry*, 3rd edn., Elsevier, Amsterdam, 1967, p. 666.
- 29 H. Park, *Bull. Chem. Soc. Jpn.*, 45 (1972) 2753.